A Centrally-Clamped Parallel-Beam Bistable MEMS Mechanism

Jin Qiu*, Jeffrey H. Lang, Alexander H. Slocum
Massachusetts Institute of Technology
* Room 3-470, 77 Massachusetts Avenue, Cambridge, MA 02139, USA
Tel: +1-617-253-1953 Fax: +1-617-258-6427 E-Mail: jqiu@mit.edu

ABSTRACT

This paper presents a monolithic mechanically-bistable mechanism that does not rely on residual stress for its bistability. The bistable mechanism comprises two centrally-clamped parallel beams that have a curved shape but no residual stress after fabrication. Modal analysis and FEA simulation of the beams are used to predict and design the bistable behavior, and they agree well. Micro-scale mechanisms are fabricated by DRIE and their test results agree well with the theoretical and numerical predictions.

INTRODUCTION

Mechanically-bistable mechanisms are useful in MEMS devices such as relays, valves, clips, threshold switches and memory cells etc. One advantage of such mechanisms is that they can apply a force to a contact during their "on" and "off" states without actuation power. Further, their hysteretic force-deflection relations offer disturbance immunity. Three categories of bistable mechanisms have been reported in the MEMS literature: latch-lock mechanisms **[1-2]**, hinged multi-segment mechanisms **[3-4]**, and residual-compressive-stress buckled-beam mechanisms **[5-8]**. A novel monolithic bistable mechanism is presented in this paper which uses no latches, no hinges, and no residual stress to achieve its bistability. This mechanism is easy to fabricate using deep reactive ion etching.

ANALYSIS AND DESIGN

The centrally-clamped parallel-beam mechanism is shown in Figure 1. It comprises two initially-cosine-shaped beams clamped together at the center. This is the shape of the mechanism as etched from a silicon wafer. At the initial position, there is no stress anywhere inside the parallel beams. When the mechanism is pushed down at the center, it will first deflect and then snap to the second stable position as shown in Figure 1.

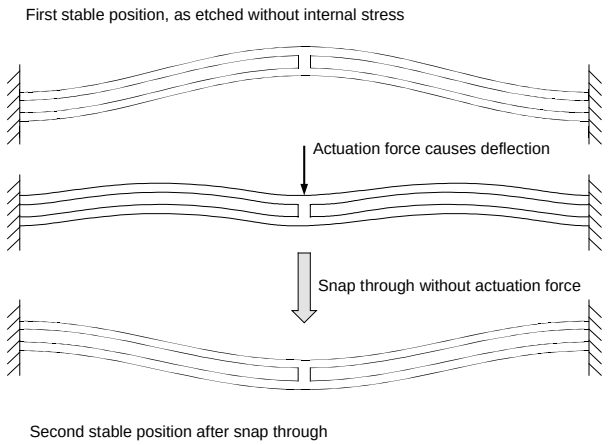

Figure 1: *The centrally-clamped parallel-beam bistable mechanism, and its deflection and snap through behavior.*

From an energy viewpoint, a single-beam mechanism with an initial cosine shape can be bistable if only its first deflection mode occurs during deflection. However, its second deflection mode will occur due to the accumulation of axial force to a critical value. The second deflection mode, which is an S-shape buckling mode, removes the energy barrier between the two stable positions of the first mode. Thus, if a single-beam mechanism is deflected to the second stable position of its first deflection mode and then released, it will always return to its original as-fabricated shape. Consequently, a single beam can not exhibit bistability without using internal stress.

The mechanism shown in Figure 1 overcomes the bistability limitation by coupling two parallel beams with a central clamp. The central clamp prevents rotation of the center of the beams **[6]**, and thus the occurrence of the second mode. Still, the third mode will develop during the deflection, but it will not lower the energy barrier as much. In this way the bistable behavior of the first deflection mode can be preserved.

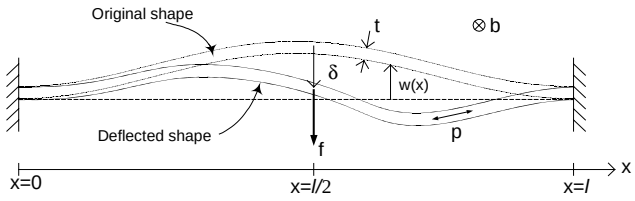

Figure 2: *Geometry and notation for beam deflection analysis.*

To analyze the bistable mechanism, consider first the single beam shown in Figure 2. It has thickness t, depth b, span l, Young's modulus E and moment of inertial $I = bt^3/12$. Let $w(x)$ denote the distance of the beam from the straight line connecting its two boundaries. Assume that the as-fabricated shape of the beam is

$$\bar{w}(x) = \bar{d}[1-\cos(2\pi x/l)]/2 \quad (1)$$

and define the normalized constant Q as

$$Q = \bar{d}/t \quad (2)$$

As the lateral force f is applied to the center of the beam at $x = l/2$, the center of the beam deflects by δ. The total length of the beam s changes too, giving rise to the axial force p. During this deflection, the beam maintains the clamped-clamped boundary conditions

$$w(0) = w(l) = 0 \quad ; \quad w'(0) = w'(l) = 0 \quad (3)$$

Following **[6]**, the beam shape during deflection can be expressed as a superposition of an infinite set of beam buckling modes, whose mode shapes are determined by the buckling equation **[9]** of an initially straight beam with the boundary conditions given by (3). To simplify this analysis, first normalize the key parameters according to

$$X = x/l \quad (4)$$

$$N^2 = p/(EI/l^2) \quad (5)$$

$$W(X) = w(Xl)/\bar{d} \quad (6)$$

Then, the shape of the beam is given by

$$W(X)=\sum_{i=0}^{\infty}A_iW_i(X) \tag{7}$$

where

$$\left.\begin{aligned}W_i(X)&=1-\cos(N_iX)\\ N_i&=2(i+1)\pi\end{aligned}\right\}\ i=0,2,4... \tag{8}$$

$$\left.\begin{aligned}W_i(X)&=1-\cos(N_iX)-2[N_iX-\sin(N_iX)]/N_i\\ N_i&=2.89\pi,4.92\pi...\end{aligned}\right\}\ i=1,3... \tag{9}$$

As fabricated,

$$\bar{W}(X)=\bar{A}_0W_0(X)\quad;\quad \bar{A}_0=0.5 \tag{10}$$

To proceed further, define the normalized parameters

$$\Delta=\delta/\bar{d}=\bar{W}(1/2)-W(1/2) \tag{11}$$

$$F=f/(EI\bar{d}/l^3) \tag{12}$$

$$S=s/(\bar{d}^2/l)=\frac{l}{\bar{d}^2}\int_0^l\sqrt{1+w'(x)^2}\,dx\approx\frac{l}{\bar{d}^2}\int_0^l(1+w'(x)^2/2)\,dx \tag{13}$$

where the latter approximation is used below,

$$\Sigma_{\max}=\varepsilon_{\max}/(t\bar{d}/2l^2) \tag{14}$$

where $\varepsilon_{\max}$ is the maximum strain during deflection,

$$U_b=u_b/(EI\bar{d}^2/l^3) \tag{15}$$

where u_b is the beam bending energy during deflection,

$$U_s=u_s/(EI\bar{d}^2/l^3) \tag{16}$$

where u_s is the beam compression energy during deflection,

$$U_f=u_f/(EI\bar{d}^2/l^3) \tag{17}$$

where u_f is the actuation energy during deflection.

The normalized parameters from (11) and are now expressed in terms of the normalized mode amplitudes, N^2, F and Q. For the deflection Δ, substitution of (7)-(10) into (11) yields

$$\Delta=2\bar{A}_0-2\sum_{j=0}^{\infty}A_{4j} \tag{18}$$

Similarly, compression can be expressed in two ways. From Hooke's Law,

$$\bar{S}-S=N^2/12Q^2 \tag{19}$$

where $\bar{S}$ is S for zero deflection. From (13),

$$\bar{S}-S=\frac{\bar{A}_0^2N_0^2}{4}-\sum_{i=0}^{\infty}\frac{A_i^2N_i^2}{4} \tag{20}$$

Maximum strain is estimated as the bending strain from the first mode plus the axial compression strain at the boundaries. Thus,

$$\Sigma_{\max}=\max[W''(X)]+N^2/6Q^2\approx W''(0)+N^2/6Q^2 \tag{21}$$

The bending energy can be expressed as

$$U_b=\frac{1}{2}\int_0^1[\bar{W}''(X)-W''(X)]^2dX=\frac{(\bar{A}_0-A_0)^2N_0^4}{4}+\sum_{i=1}^{\infty}\frac{A_i^2N_i^4}{4} \tag{22}$$

where the last equality uses (7)-(10). For a given N, the compression energy is expanded as a Taylor series according to

$$\begin{aligned}U_s&=U_s\big|_{S=S_0}+\left.\frac{dU_s}{dS}\right|_{S=S_0}(S-S_0)=U_s\big|_{S=S_0}-N^2(S-S_0)\\ &=U_s\big|_{S=S_0}-N^2(\bar{S}-S_0)+N^2(\bar{S}-S)\equiv C_s+N^2(\bar{S}-S)\\ &=C_s+N^2(\frac{\bar{A}_0^2N_0^2}{4}-\sum_{i=0}^{\infty}\frac{A_i^2N_i^2}{4})\end{aligned} \tag{23}$$

where the second equality results from the relation between the energy and force of the compressing spring, and C_s is a constant. Similarly, the actuation energy can be expressed by

$$U_f=C_f-F(2\bar{A}_0-2\sum_{j=0}^{\infty}A_{4j}) \tag{24}$$

The total energy within the mechanism U_t is the sum of (22), (23) and (24) so that

$$\begin{aligned}U_t=C_t&+[\frac{N_0{}^4(A_0^2-2A_0\bar{A}_0)}{4}-\frac{N^2A_0^2N_0^2}{4}+2FA_0]\\ &+(\sum_{i=1}^{\infty}\frac{N_i{}^4A_i^2}{4}-\sum_{i=1}^{\infty}\frac{N^2A_i^2N_i{}^2}{4}+2F\sum_{j=1}^{\infty}A_{4j})\end{aligned} \tag{25}$$

where C_t is a constant. The mode amplitudes should minimize U_t, thus

$$\partial U_t/\partial A_i=0 \tag{26}$$

Applying (26) to (25) yields

$$A_0=-\bar{A}_0\frac{N_0^2}{N^2-N_0^2}+\frac{4F}{N_0^2(N^2-N_0^2)} \tag{27}$$

$$A_{4j}=\frac{4F}{N_{4j}^2(N^2-N_{4j}^2)}\ ,\quad \text{j=1,2,3...} \tag{28}$$

$$(N^2-N_k^2)A_k=0\ ,\quad k=1,2,3,5,6,7... \tag{29}$$

Thus, the deflection mode amplitudes are determined in terms of N^2 and F.

During beam deflection, N^2 increases from zero to N_k^2 for the lowest permissible k. It then remains at N_k^2 due to the free development of the corresponding A_k as indicated by (29). Other than the case $N^2=N_k^2$, A_k is always zero, also as indicated by (29). For the single beam case, *k = 1*, but for the centrally-clamped parallel beam case, $k=2$ because A_1 is constrained to zero by the clamp at the center of the parallel beams.

Substituting (27)-(29) into (20) and equating the result to (19) yields

$$\begin{aligned}&\frac{4}{N_0^2}[1+\sum_{j=1}^{\infty}\frac{N_0^2(N^2-N_0^2)^2}{N_{4j}^2(N^2-N_{4j}^2)^2}]F^2-2\bar{A}_0N_0^2F\\ &+[\frac{N^2(N^2-N_0^2)^2}{12Q^2}-\frac{\bar{A}_0^2N_0^2(N^4-2N^2N_0^2)}{4}]=0\end{aligned} \tag{30}$$

for $N<N_k$, and for $N=N_k$,

$$\begin{aligned}&\sum_{j=0}^{\infty}\frac{4}{N_{4j}^2(N_k^2-N_{4j}^2)^2}F^2-\frac{2\bar{A}_0N_0^2}{(N_k^2-N_0^2)^2}F\\ &+[\frac{N_k^2}{12Q^2}-\frac{\bar{A}_0^2N_0^2(N_k^4-2N_k^2N_0^2)}{4(N_k^2-N_0^2)^2}+\frac{A_k^2N_k^2}{4}]=0\end{aligned} \tag{31}$$

Finally, (30) and (31) can be used to determine F from N^2 and A_k, respectively; in order to have a real solution for F for (31),

$$Max(A_1^2)=0.119-0.333/Q^2 \tag{32}$$

$$Max(A_2^2)=0.062-0.333/Q^2 \tag{33}$$

Following this, (7) with (27)-(29) can be used to determine the beam shape and hence Δ from F. Throughout, the beam parameters enter this analysis only through Q. To illustrate these results, the force-deflection relation at X = *1/2* is shown in Figure 3 for different values of Q.

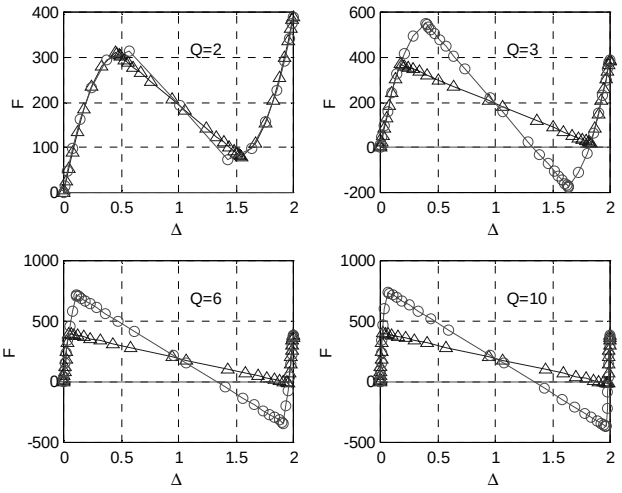

***Figure 3**: F-Δ relations for different Q; triangles are for the single beam (k = 1) in which mode i=1 is free, circles are for a centrally-clamped parallel beams (k = 2) in which mode i=1 is constrained.*

From the preceding analysis, it is apparent that the force-displacement relation is determined only by *Q*. Moreover, when *Q* is large enough, all characteristics of this relation for the centrally-clamped parallel beams are asymptotic to constants. For example, for approximately $Q \equiv \bar{d}/t \geq 6$,

$$f_{top} \approx 758\ EI\bar{d}/l^3 \quad ; \quad \delta_{top} \approx 0.03\bar{d} \tag{34}$$

$$f_{bottom} \approx -384\ EI\bar{d}/l^3 \quad ; \quad \delta_{bottom} \approx 1.99\bar{d} \tag{35}$$

$$\delta_{zero} \approx 1.33\ \bar{d} \tag{36}$$

$$\varepsilon_{\max} \approx 2450\%\ t\bar{d}/l^2 \tag{37}$$

where f_{top} and f_{bottom} are the peak forces required to achieve snap through in the negative and positive directions, respectively, δ_{top} and δ_{bottom} are the deflections at which these forces occur, respectively, δ_{zero} is the deflection at which the force is zero, and $\varepsilon_{\max}$ is the maximum strain experienced by the beam during its entire travel. These results are used to guide the design of the force-deflection relation of the clamped parallel-beam center, and the maximum stress in the mechanism.

Nonlinear finite element analysis (FEA) agrees well with the modal analysis. A comparison of the force-displacement relation at the center of the experimental mechanism obtained through modal analysis and FEA is shown in Figure 6.

FABRICATION AND TEST

Micro-scale centrally-clamped parallel-beam bistable mechanisms have been fabricated and successfully tested. The mechanism described below has been designed with a span of *l = 3 mm*, a thickness of *t = 10 μm*, a depth of *b = 480 μm* and an initial apex height of $\bar{d}$ = 60 *μm*. The estimated maximum strain within the mechanism during snap through is 0.16%.

The experimental mechanism was fabricated by deep reactive ion etching (DRIE) through a silicon wafer. In its etch mask, fillets were added at the sharp corners to lower the stress concentration. Further, a halo was included in the mask, so that the etch space has the same width throughout the mask. This arrangement ensures that etching occurs at the same rate at all locations.

The etch mask itself comprised a *0.75 μm* oxide hard mask, and a *15 μm* photoresist soft mask. The etch recipe "MIT69A" was used as developed in the Microsystems Technology Laboratories of MIT. The total time taken to etch through the whole wafer thickness of *480 um* was about 4.5 hours. To smooth out the sidewall surface roughness created during DRIE, a dry isotropic etch using SF_4 for 15 seconds follows the through etch. This technique **[10]** can significantly increase the fracture stress of a DRIE structure.

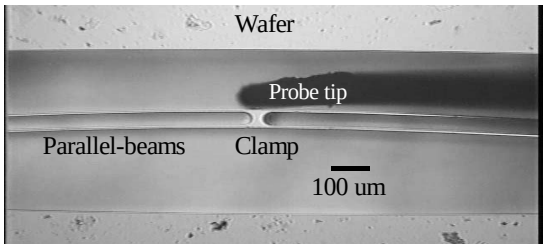

***(a)** The mechanism as etched; the probe is ready to push.*

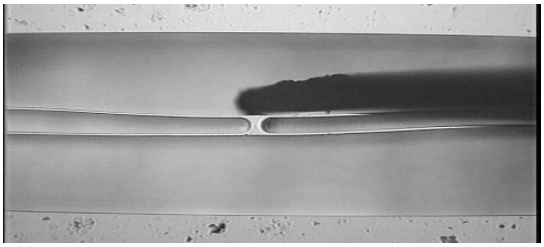

***(b)** Deflection as the probe pushes the mechanism.*

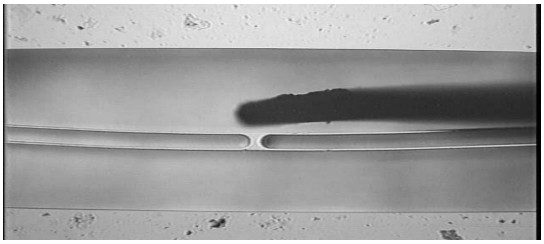

(c) *The mechanism snaps to its second stable position after being pushed. The probe tip and the parallel-beams are separated.*

***Figure 4:** A bistable mechanism fabricated with DRIE.*

A micro probe is used to push the experimental mechanism down and up at its center clamp. The two bistable positions of the mechanism, together with a middle position while being pushed down, are shown in Figure 4. The mechanism has the dimensions stated in Figure 6, but only the center portion of the mechanism is shown in Figure 4. However, as observed with a microscope, the fabricated beams have a tapered shape as a result of the DRIE process. The top thickness is *8 μm* and the bottom thickness is 22 *μm*, while the designed thickness is *10 μm*.

To measure the force-deflection characteristics of the experimental bistable mechanisms, a specialized MEMS flexure tester **[11]** was developed. The tester, shown in Figure 5, features a resolution of *10 nm* for the displacement, and 100 *μN* for the force.

Using the tester, the force-deflection relation of the bistable mechanism shown in Figure 4 was measured. The results are shown in Figure 6, and these results are compared to both the modal analysis developed above and FEA. To accommodate the actual tapered beam geometry, the average thickness of *15 μm* was used for the modal analysis and FEA. The measured parallel-beam force-deflection relation matches the modal analysis and FEA well. The difference between them is believed to be from 2-D modeling simplifications and fabrication variations.

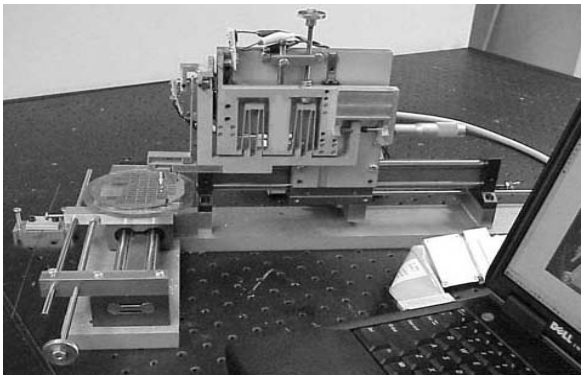

Figure 5*: The specialized MEMS flexure stiffness tester.*

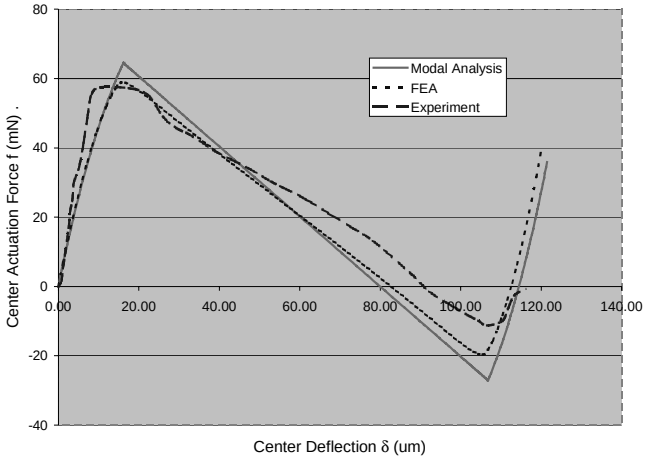

Figure 6*: Quasistatic force-deflection relation of the experimental mechanism from modal analysis, FEA, and experiment. The etched beams have an 8 μm top thickness, a 22 μm bottom thickness, a 60 μm initial apex height, a 3 mm span, and a 480 μm depth. For the modal analysis and FEA, an average 15 μm thickness of each beam is assumed.*

SUMMARY AND CONCLUSIONS

This paper has proposed, analyzed, designed and fabricated a bistable mechanism that does not rely on hinges, latches or as-fabricated internal stress for its bistability. The mechanism comprises only a pair of initially-cosine-shaped parallel beams that are clamped together at their centers. Such a mechanism appears to be well suited for use in applications such as relays, valves, clips etc. Further, it should be possible to extend the mechanism to two dimensions in the form of initially curved but parallel plates.

A buckling-beam analysis of the mechanism was used to support its design. This analysis resulted in a relation between the force applied to, and the deflection of, the center of the mechanism. It is interesting to note that the character of this relation is dependent only on the single parameter Q when the beam deflections are properly normalized. Because of this, two important general observations can be made. First, the mechanism exhibits bistability only for $Q > 2.4$. This can be observed in Figure 3. For the case of $Q = 2$, f_{bottom} is positive for $k = 2$, hence the mechanism is not bistable. For the other cases of $k = 2$, which all have $Q \geq 3$, the beam is bistable. Note too that f_{bottom} is never significantly negative for the single beam case of $k = 1$ and so the single beam is never bistable from a practical viewpoint. Second, for $Q \geq 6$, approximately, the character of the force-deflection relation has essentially reached the asymptotic character described by (34)-(37). Therefore (34)-(37) serve as useful design tools.

Finally, experimental micro-scale mechanisms were fabricated from single-crystal silicon wafers using deep reactive-ion etching. The mechanisms exhibited the expected bistability. Further, the details of their force-deflection relations were well matched to those predicted by the buckling beam analysis, which were in turn both well matched to those predicted by FEA. This demonstrates the validity of the analysis and the general observations made above.

ACKNOWLEDGEMENT

The work reported here was supported by ABB. Fabrication was performed in the Microsystems Technology Laboratories of MIT. The authors wish to thank Prof. Martin Schmidt of MIT, Dr. Ralf Struempler and Dr. Dagfin Brodtkorb of ABB for helpful discussion during the course of this work. We also wish to acknowledge the help of Joachim Sihler, Victoria Sturgeon, Jian Li, Micah Smith, Carolyn Phillips and James White of MIT during the development of the MEMS stiffness tester.

REFERENCES

1. M Hoffmann et al, "All-silicon bistable micromechanical fiber switch based on advanced bulk micromachining", *IEEE Journal on Selected Topics in Quantum Electronics*, Vol 5:1, 46–51, 1999.
2. X-Q Sun et al, "A bistable microrelay based on two-segment multimorph cantilever actuators", *Proc MEMS 98*, 154 –159.
3. B Jensen et al, "Design of two-link, in-plane, bistable compliant micro-mechanisms", *J Mech Design*, 121:3, 416-423, 1999.
4. EJJ Kruglick et al, "Bistable MEMS relays and contact characterization", *Proc SSSA Workshop*, 333-337, 1998.
5. M Taher, "On a tunable bistable MEMS-theory and experiment", *J MEMS*, Vol 9:2, 157 –170, 2000.
6. M Vangbo, "Analytical analysis of a compressed bistable buckled beam", *Sensors and Actuators A*, 69:3, 212-216, 1998.
7. Y-J Yang et al, "Testing and characterization of a bistable snapping microactuator based on thermo-mechanical analysis", *Proc SSSA*, Vol 2, 337–340, 1995.
8. B Wagner et al, "Bistable microvalve with pneumatically coupled membranes", *Proc MEMS 96*, 384 –388.
9. S Crandall et al, *An Introduction to the Mechanics of Solids*, 2nd edition, McGraw-Hill, 583-590.
10. K-S Chen et al, "Silicon strength testing for mesoscale structural applications", *MRS Spring Meeting Symposium*, N3.8.
11. J Qiu et al, "An instrument to measure the stiffness of MEMS mechanisms", to appear in *Proc 10th International Conference on Precision Eng*, July 2001, Yokohama Japan.